αCT1 Peptide Sensitizes Glioma Cells to Temozolomide in a Glioblastoma Organoid Platform

Jingru Che[1], Thomas J. DePalma[1], Hemamylammal Sivakumar[1], Louisa S. Mezache[1], Miranda M. Tallman[2], Monica Venere[3], Katelyn Swindle-Reilly[1], Rengasayee Veeraraghavan[1], and Aleksander Skardal[1]

[1]The Ohio State University
[2]The Ohio State University Wexner Medical Center
[3]The Ohio State University Comprehensive Cancer Center

April 29, 2022

Abstract

Glioblastoma (GBM) is the most common form of brain cancer. Even with aggressive treatment, tumor recurrence is almost universal and patient prognosis is poor because many GBM cell subpopulations, especially the mesenchymal and glioma stem cell populations, are resistant to temozolomide (TMZ) the most commonly used chemotherapeutic in GBM. For this reason, there is an urgent need for the development of new therapies that can more effectively treat GBM. Several recent studies have indicated that high expression of connexin 43 (Cx43) in GBM is associated with poor patient outcomes. It has been hypothesized that inhibition of the Cx43 hemichannels could prevent TMZ efflux and sensitize otherwise resistance cells to the treatment. In this study, we use a 3-dimensional organoid model of GBM to demonstrate that combinatorial treatment with TMZ and αCT1, a Cx43 mimetic peptide, significantly improves treatment efficacy in certain populations of GBM. Confocal imaging was used to analyze changes in Cx43 expression in response to combinatorial treatment. These results indicate that Cx43 inhibition should be pursued further as an improved treatment for GBM.

1. Introduction

Glioblastoma (GBM) is an aggressive, terminal cancer in the brain. It is a lethal and heterogeneous disease, and even with maximally aggressive surgery and chemoradiotherapy, median survival for GBM patients is 14.5 months (Stupp et al., 2005). These tumors infiltrate the brain, are surgically incurable, and universally recur. Upon recurrence, response rates to standard treatment are less than 5%, leading to a median survival of 8 months (Taal et al., 2014). Despite advances in managing other types of cancer, only 4 new treatments have been FDA-approved for GBM in the last 3 decades. A major challenge in translating successful therapies into the clinic is modeling the genetic, epigenetic, and micro-environmental heterogeneity of GBMs, as well as accounting for the blood brain barrier (BBB) (Rybinski & Yun, 2016). GBMs evolve spontaneously and in response to treatment, making selection of patient-specific therapies a challenge (Malkki, 2016; Sottoriva et al., 2013). Seminal studies employing multiple biopsies of single patients' tumors have shown that multiple distinct GBM molecular subtypes (i.e. classical, proneural, and mesenchymal) exist within the same tumor, although these designations are now questioned due to little clinical improvements based on subtyping (Sottoriva et al., 2013; Tang et al., 2015). Alternatively, glioma stem cell (GSC) subpopulations have arisen as a key cell type of interest due to their ability to evade therapy and drive tumor recurrence (Auffinger et al., 2015; Heimberger et al., 2003; Swartz et al., 2014). Often, recurring tumors, while still heterogeneous, display increased presence of the mesenchymal and GSC subpopulations which correlate with poor prognosis, heightened inflammation, matrix metalloproteinase (MMP) expression, and ECM remodeling – factors that further drive tumor progression (Fedele et al., 2019; Segerman et al., 2016).

Precision medicine has largely failed to improve clinical outcomes in GBM. Precision medicine utilizes genomic and molecular profiling of tumors to identify drugs for treatment of patients' tumors. In neuro-oncology, this approach fails to incorporate important contributions of the BBB. The current approach in neuro-oncology is to limit drug selection to the few agents that are known to cross the BBB. However, this may be overly restrictive, particularly given historical examples of agents that have been thought not to be able to penetrate BBB (i.e. rituximab) that are known to be effective against GBM tumor cells (Rubenstein et al., 2013). Thus, precision medicine in neuro-oncology will require additional understanding of how the tumor and surrounding microenvironment influence BBB integrity, BBB permeability, and drug delivery. Yet, due to the inability to assess BBB-tumor interplay more effectively, temozolomide (TMZ), a BBB-permeable alkylating agent that damages DNA and induces tumor cell apoptosis, remains the ubiquitous chemotherapy for GBM patients. Clinically – and recapitulated by our bioengineered tumor organoids – there is often a correlation between clinical biomarkers such as MGMT (O^6-methylguanine-DNA methyltransferase) promoter methylation and IDH (isocitrate dehydrogenase) mutational status and patient (or organoid) TMZ response (Verhaak et al., 2010). In patients that do not respond to TMZ, regardless of MGMT or IDH status, alternative treatments, including strategies involving TMZ sensitization, need to be investigated.

As noted above, TMZ is the most widely used GBM chemotherapy agent due to its unique ability to pass the BBB. However, some tumor cells are able to evade TMZ via drug efflux mechanisms that expel TMZ from the cell before DNA is damaged. Mounting evidence implicates connexin 43 (Cx43) hemichannels in drug efflux underlying chemotherapy-resistance, and Cx43 hemichannel inhibition has been shown to sensitize GSCs to TMZ (Grek et al., 2018; Murphy et al., 2016). However, available evidence comes from simple two-dimensional (2D) cell line cultures lacking the heterogeneity and complexity of tumor and brain physiology. Another key barrier to clinical translation is that Cx43 hemichannel inhibitors, such as the Cx43-mimetic peptides αCT1 and αCT11, cannot cross the BBB, necessitating local delivery at the tumor site sustained over extended periods (months) (Grek et al., 2018; Murphy et al., 2016). Previous nanoparticle-based delivery approaches have been limited to 2-3 weeks, but sustained release technologies have great potential to increase local sustained delivery of these peptides (Roberts et al., 2020). New model systems that recapitulate 3D *in vivo* human brain physiology, support the heterogeneity of GBM, and provide direct experimental manipulation and observation – such as tumor organoids – could be used to evaluate and optimize combinatorial therapies such as this.

Here we evaluate the potential of two Cx43-mimetic peptides, αCT11 and αCT1, to inhibit Cx43 hemichannels and sensitize GSCs and other GBM cells populations to TMZ in a 3D hyaluronic acid (HA) and collagen hydrogel-based tumor organoid system that we have deployed across a variety of tumor types, including mesothelioma, melanoma, lung adenocarcinoma, colorectal carcinoma, sarcoma, appendiceal, adrenocortical carcinoma, and gliomas (Forsythe et al., 2019; Maloney et al., 2020; Mazzocchi et al., 2019; Mazzocchi et al., 2018; Votanopoulos, Forsythe, et al., 2019; Votanopoulos, Mazzocchi, et al., 2019; Votanopoulos & Skardal, 2020). The results of the current study demonstrated that αCT11 had no statically significant effect on the viability of TMZ treated organoids. However, combinatorial treatment with TMZ and αCT1 shows increased efficacy in certain GBM cell populations compared to the TMZ-only treatment. Particularly, the GSCs that are often responsible for clinical chemotherapy-resistance, showed a drastic decrease in viability after the combinatorial treatment. Immunofluorescence microscopy indicated that Cx43 is expressed in all tested cell lines, and αCT1 increases the number of Cx43 aggregates in GBM cell lines that responded to the combinatorial treatment, which may indicate that αCT1 affects Cx43 production as well as hemichannel function. These studies provide an early indication that Cx43 hemichannel inhibition may be an effective therapy to increase TMZ efficacy, sensitizing GBM populations to TMZ with αCT1 could enable remission in patients with lower chance of tumor recurrence.

2. Materials and Methods

2.1. Cell Culture-GBM Cell Lines

There are multiple distinct subpopulations that have been shown to respond differently to radiation and treatment with TMZ (Lee, 2016). Three GBM cell lines were employed in order to compare how different

populations of cells respond to the treatment in GBM organoids. GBM cell lines U-87 MG (ATCC® HTB-14™), A172 (ATCC® CRL-1620™) (obtained from ATCC, Manassas, VA), and BT169 (ATCC®CRL-3413) were employed. Each cell line was cultured separately. U-87 MG and A172 cancer cell lines were cultured in high glucose Dulbecco's Modified Eagle Medium (DMEM) with 10% fetal bovine serum (FBS), 1% L-glutamine, and 1% penicillin/streptomycin in a tissue culture incubator at 37degC with 5% CO_2. B169 cell line was cultured in NeuroCult Basal Medium with proliferation Supplement, 20 ng/mL EGF, 20 ng/mL β-FGF and 2 µg/mL heparin sulfate in a tissue culture incubator at 37°C with 5% CO_2.

2.2. Patient-Derived GBM Cells

GBM 3691 cells were obtained as de-identified specimens that were initially acquired as primary human brain tumor patient specimens in accordance with appropriate, approved Institutional Review Board (IRB) protocols. GBM 3691 was a kind gift from Dr. Jeremy Rich (University of Pittsburgh; IRBs from Duke University and The Cleveland Clinic; transferred via MTAs). Cells were cultured in suspension at 37°C at 5% CO_2 in Neurobasal media (minus phenol red; Gibco) with added B27 (minus Vitamin A; Gibco), human fibroblast growth factor-2 (10 ng/mL; Miltenyi Biotec), human epidermal growth factor (10 ng/mL; Miltenyi Biotec), L-glutamine (2 mM; Gibco), sodium pyruvate (1 mM; Gibco), and penicillin/streptomycin (100 I.U./ml/100 ug/ml; Gibco). Prior to seeding within hydrogels, cell aggregates are dissociated into a single cell suspension using TrypLE (Gibco).

2.3. GBM Organoid Fabrication

Bioengineered hydrogels are a widely used tool in the tissue engineering field. They serve as a biomimetic scaffold that supports cells and can deliver a wide range of bioactive agents to the embedded cells. The hydrogel used in these studies is composed of thiolated-hyaluronic acid (HA), thiolated-gelatin, and poly-ethylene glycol diacrylate (PEGDA) dissolved in water containing 0.1% w/v photoinitiator (Irgacure 2959) to a final concentration of 1%w/v. The 3 components are combined in a 2:2:1 ratio (HA:Gelatin:PEGDA) by volume. Cells are then suspended within the solution at a concentration of 5 million cells/ml. A 10 µL droplet of hydrogel solution is pipetted onto each well of a PDMS coated 48-well resulting in organoid constructs containing 50,000 cells per organoid. The organoids are then cured with 365nm wavelength UV light for 2 seconds.

2.4. Combinatorial Temozolomide and Peptide Treatment

Temozolomide (TMZ) is an anti-cancer drug that is commonly used in chemotherapy to treat brain cancer. TMZ is an alkylating agent prodrug, delivering a methyl group to purine bases of DNA (Zhang et al., 2012). TMZ was purchased from SelleckChem (Houston, TX). Two Cx43 mimetic peptides, [?]CT1 and [?]CT11 (LifeTein, Somerset, NJ) were evaluated in this experiment. Different combinations of TMZ and αCT1 or αCT11 concentrations were tested in each cell line to determine the optimal combination. Organoids are treated with combinations of TMZ (0, 10, 100, or 1000 µM) and αCT11 (0, 4, 40, 400 µM) or αCT1 peptide (0, 1, 10, 100 µM) for 7 days, with the drugs and peptide replenished on day 4. TMZ and peptide were dissolved in media and added directly to the organoids.

2.5. Organoid Viability Analysis

After the organoids were treated for 7 days, the viability was assessed by Live/Dead imaging and quantitatively validated with ATP Luminescent assay (Cell Titer-Glo 3D®, Promega). Luminescence level is proportional to the number of viable cells, thus reflects the level of activity in an organoid. The assay was conducted per the vendor protocol. Briefly, media was removed from the well and replaced with 200 µL of assay solution (100 µL of CellTiter-Glo® 3D Reagent mixed with 100 µL DMEM). The plate was then mixed vigorously on a plate shaker for 5 minutes at 100 rpm followed by incubation at room temperature for an additional 25 minutes. 180 µL of the mixture from each well was transferred to a white flat bottom Polystyrene 96 well plate. Luminescence was measured using a microplate reader (Varioskan LUX, ThermoFisher).

LIVE/DEAD staining was performed on day 7 of organoid culture. Calcein AM (excitation and emission ˜495/515 nm, 1:2000 dilution) and Ethidium Homodimer-1 (EthD-1) (excitation/emission 528/617 nm, 1:500

dilution) were dissolved in 200 µL of a PBS and DMEM mixture (1:1), and introduced to each organoid with a 30-minute culture. Fluorescent imaging was performed using Nikon A1R Confocal live cell confocal microscope (CMIF, OSUCCC). Z-Stacks were obtained for each organoid and presented as maximum intensity projections.

2.6. αCT1 Peptide-Cx43 Interaction

αCT1 peptide conjugated with Fluorescein isothiocyanate (FITC- αCT1; LifeTein) was used to visualize the distribution of αCT1 peptide inside the cells during treatment. Four experimental groups were used: control (no drug or peptide), TMZ (100 µM), FITC-αCT1 (100 µM), and combination of 100 µM TMZ and 100 µM FITC-αCT1. Treatment was added 24 hours after seeding the organoids and replenished on day 4, the organoids were fixed with 4% PFA for 1 hour on day 7. Constructs were stained as described in section 2.7 for Cx43.

2.7. Immunostaining and Confocal Imaging

Organoids were fixed for 1 hour at room temperature with 4% PFA. Samples were then blocked for 1 hour at room temperature using goat blocking solution (5% Normal Goat Serum with 0.1% w/v Sodium Azide) with 0.1% Triton-X. Primary antibodies (anti-Connexin 43 N-terminal antibody purchased from Sigma-Aldrich), were diluted in goat blocking solution and samples are incubated overnight at 4°C. Samples were then washed with PBS 3 times for 5 minutes each. Secondary antibodies were also diluted in goat blocking solution and incubated with samples overnight at 4°C. Samples were then washed with PBS 3 times for 5 minutes and stained with DAPI (NucBlue, Invitrogen) and Allexa-647 conjugated Phalloidin (Invitrogen) per the manufacturer instruction. Imaging was conducted using Nikon A1R HD Confocal Microscope.

2.8. Statistical Analysis

ATP luminescence data (n=4) was averaged after subtracting blank values and analyzed in GraphPad Prism. Two-Way ANOVA with confidence intervals of 95% followed by a multiple comparisons test (Tukey) was used to analyze the combinatorial treatment studies.

3. Results

3.1. 3D GBM Hydrogel Organoid Fabrication and Drug Treatment Workflow

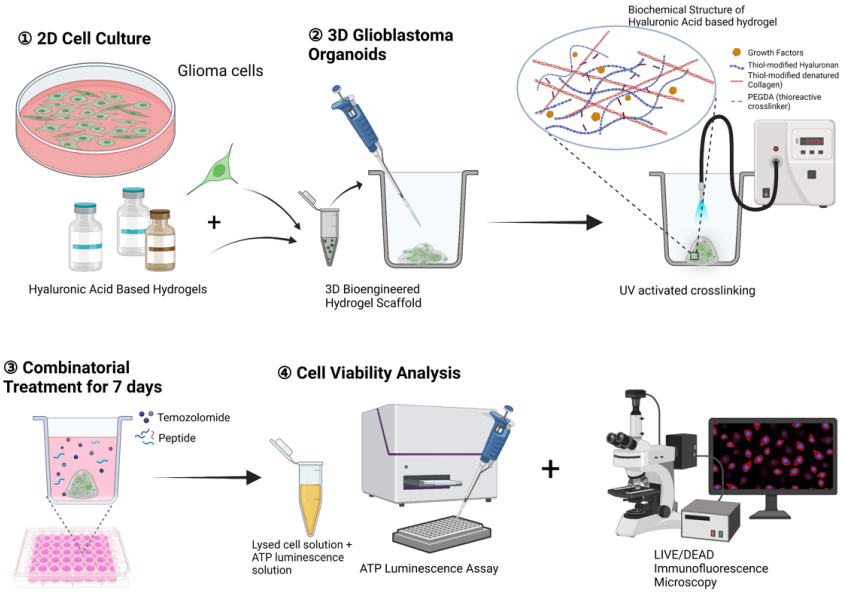

Figure 1. Schematic describing the overall workflow of the study. Tumor cells are expanded on culture plastic and passage with Trypsin (1). The cells are then suspended in hydrogel solution. 10mL droplets are pipetted into a well plate and crosslinked with UV light for 2 seconds (2). After 24 hours, drug treatment is started (3). Constructs are then analyzed for viability and Cx43 protein expression (4).

Previous work from our lab and others has shown that cancer cells grown in 3D hydrogels retain more properties of *in vivo* tumor cells (Devarasetty et al., 2020; Forsythe et al., 2019; Mazzocchi et al., 2018; Votanopoulos, Forsythe, et al., 2019; Votanopoulos, Mazzocchi, et al., 2019). For that reason, we have chosen to test the effect of the combinatorial treatments on cells grown in 3D hydrogel constructs instead of on traditional flat 2-dimension cell culture plastic. GBM tumor cells are encapsulated within the hydrogel solution, which is comprised of thiolated-HA, thiolated-gelatin, and polyethylene glycol diacrylate (PEGDA) in a 2:2:1 ratio. Six organoids were generated for each treatment group, including four organoids used for ATP assay and two for LIVE/DEAD imaging. Drug treatment proceeds for 7 days at which point, cell viability is assessed, or the samples are fixed for immunostaining. The hydrogel is also optically transparent which allows for analysis via confocal microscopy. See **Figure 1** for a detailed outline of the workflow used in the studies presented here.

3.2. δμβινατοριαλ τρεατμεντ ωιτη TMZ ανδ α̃T11 δοες νοτ ινςρεασε ΓBM ςελλ κιλλινγ.

To test efficacy of Cx43 targeting in combination with TMZ, we first investigated the effect of αCT11 peptide on drug efficacy.Organoids were treated with combinations of TMZ (0, 10, 100, 1000 μM) and αCT11 (0, 4, 40, 400 μM) with the drug and media replenished after 4 days. After combinatorial treatment of GBM organoids for 7 days. Cell viability was assessed using the CellTiter Glo 3D (Promega) assay. The assay is used to quantify ATP levels in cells and has been previously verified for studying the drug efficacy of 3D cancer organoids (Dominijanni et al., 2021). Live/dead staining was used to qualitatively confirm results from the viability assay. These images can be found in**Supplemental Figures 1-3** . The GBM organoids were grouped by three concentrations of TMZ (10, 100, or 1000 μM) and a control group (TMZ = 0), and the organoid viability is compared across three concentrations of αCT11 (4, 40, or 400 μM) and a control group ([αCT11] = 0) in each TMZ subgroup.

The viability of all 3 GBM cell lines decreased as TMZ concentration increased (**Figure 2**). In A172 and BT169 organoids, there is no statistically significant difference between cells treated with TMZ alone and αCT11 (**Figure 2A and 2C**). The U87 organoids showed significantly decreased viability in the TMZ 10 μM + αCT11 4 μM condition, but in no other condition (**Figure 2B**).

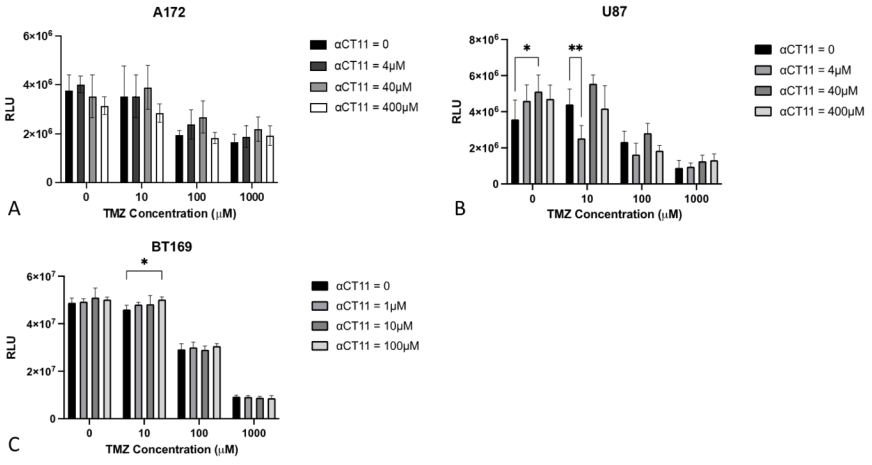

Φιγυρε 2. ΑΤΠ ασσαψ ρεσυλτς οφ ςελλ λινες τρεατεδ ωιτη α̃T11 ανδ TMZ .A , A172 cell line viability after treatment with TMZ at 0, 10, 100, or 1000 μM alone or in combination with αCT11

at concentrations of 0, 4, 40, 400 μM .**B** , U87 cell line ATP data viability after treatment with TMZ at 0, 10, 100, 1000 μM alone or in combination with αCT11 at concentrations of 0, 4, 40, 400 μM .**C** , BT169 cell line viability after treatment with TMZ at 0, 10, 100, 1000 μM alone or in combination with αCT11 at concentrations of 0, 1, 10, 100 μM .

3.3. αCT1 συγγεσσφυλλψ σενσιτιζες ΓΒΜ οργανοιδς το τεμοζολομιδε

Like αCT11, αCT1 is a Cx43 mimetic peptide. However, unlike αCT11, it contains a cell penetration sequence that should allow it to better permeate the cells (Jiang et al., 2019). We hypothesized that because of the presence of this additional sequence, it would significantly increase GBM cell sensitivity to TMZ compared to αCT11. Using an ATP assay to quantify cell viability, we found that when the αCT1 peptide is present at high concentrations (αCT1 = 10 and 100 μM) in A172 and BT169 organoids, viability is considerably decreased compared to the control groups (αCT1 = 0) for several TMZ concentrations (**Figure 3A and 3C**). Surprisingly, αCT1 peptide at a concentration of 10 μM is more effective in the A172 organoids than the highest concentration (100 μM). In the U87 MG organoids, however, the αCT1 had little influence on cell growth (**Figure 3B**).

The LIVE/DEAD images (**Figure 4**) show comparable results as the ATP assay. The highest concentration of TMZ (1000 μM) combined with highest concentration of αCT1 (100 μM) indicates the most significant cell killing in A172 and BT169 cell lines (**Figure 4A and 4C**). This combination of TMZ and αCT1 treatment group, however, did not increase cell killing efficacy in the U87 cell line, which is consistent with the results of the ATP assay (**Figure 4B**). LIVE/DEAD images of combinatorial treatment with TMZ and lower concentrations of αCT1 (1 and 10 μM) are shown in **Supplemental Figures 4-6** .

This finding indicates that the combinatorial treatment with TMZ and αCT1 may only be effective in certain GBM tumor populations. It's also worth noting that even when the TMZ concentration is zero, αCT1 shows a significant decrease in viability in the A172 organoids. This could indicate that αCT1 is impacting several important cell pathways, not just those related to TMZ efficacy in GBM cells.

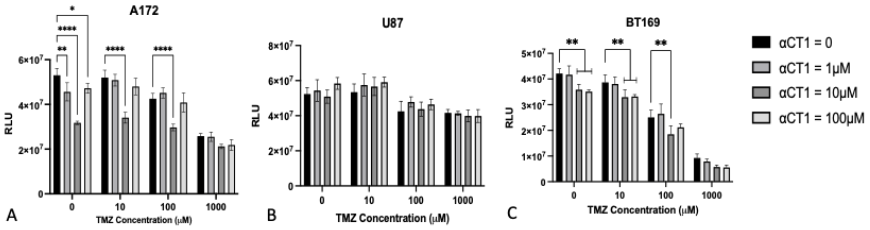

Φιγυρε 3. ΑΤΠ ασσαψ ρεσυλτς οφ χελλ λινες τρεατεδ ωιτη αCT1 ανδ TMZ. A , A172 cell line viability after treatment with TMZ at 0, 10, 100, or 1000 μM alone or in combination with αCT11 at concentrations of 0, 1, 10, 100 μM. **B** , U87 cell line ATP data responding t viability after treatment with o TMZ at 0, 10, 100, 1000 μM alone or in combination with αCT1 at concentrations of 0, 1, 10, 100 μM.**C** , BT169 cell line viability after treatment with TMZ at 0, 10, 100, 1000 μM alone or in combination with αCT1 at concentrations of 0, 1, 10, 100 μM.

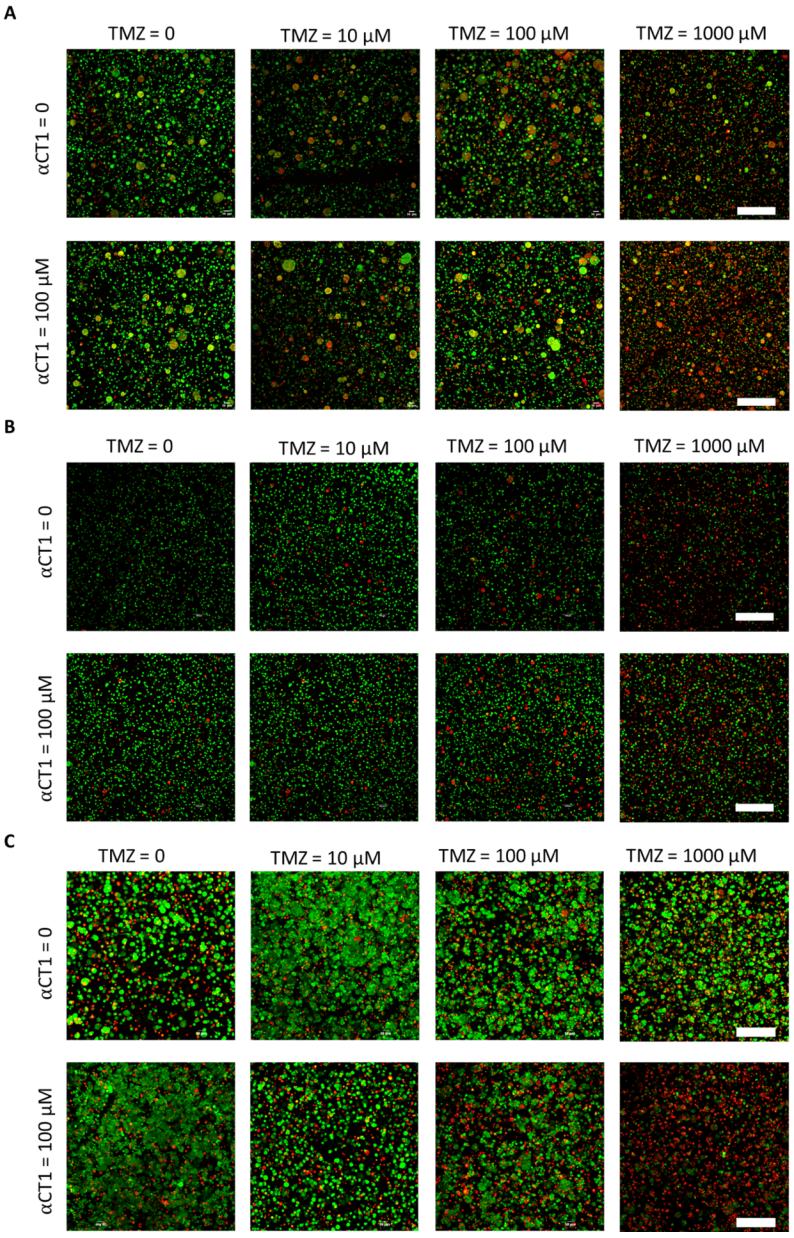

Φιγυρε 4. ΛΙΎΕ/ΔΕΑΔ ιμαγες οφ τηρεε τεστεδ ςελλ λινες ωιτη διφφερεντ ςομβινατιονς οφ αˆT1 (0 ανδ 100 μM) ανδ TMZ (0, 10, 100, 1000 μM). A, LIVE/DEAD images of A172. **B** , LIVE/DEAD images of U87.**C** , LIVE/DEAD images of BT169. Green – Calcein AM-stained viable cells; Red – Ethidium homodimer-1-stained dead cell nuclei. Scale bar – 250 μm. LIVE/DEAD images of samples treated with 1 and 10 μM αCT1 can be found in Supplemental Figures 4-6.

3.4 Confocal imaging shows that combination treatment induces changes in Cx43 expression and intracellular distribution.

To better understand the mechanism of αCT1 enhanced cell killing, we repeated the treatment in A172, U87, and BT169 cell lines using a fluorescence conjugated αCT1 (FITC-αCT1) combined with TMZ. The interaction between FITC-αCT1 and N-terminal Cx43 was visualized under the confocal microscope. The

complete procedure can be found in sections 2.6 and 2.7.

As shown in **Figure 5** , Cx43 level did not show significant changes after the TMZ (100 µM), or FITC-αCT1 (100 µM) treatment in any of the three cell lines. However, in A172 and BT169 cell lines (**Figure 5A and 5B**), the combination of 100 µM TMZ and 100 µM FITC-αCT1 treatment group significantly increased the number of Cx43 aggregates as well as the Cx43 signal intensity compared to the U87 cell line, which only exhibits a slight increase in the Cx43 aggregates number within the cell bodies (**Figure 5C**). This observation indicates that FITC-αCT1 combined with TMZ may induce changes in TMZ- related signaling pathways and affect Cx43 protein functions and activities in GBM cells.

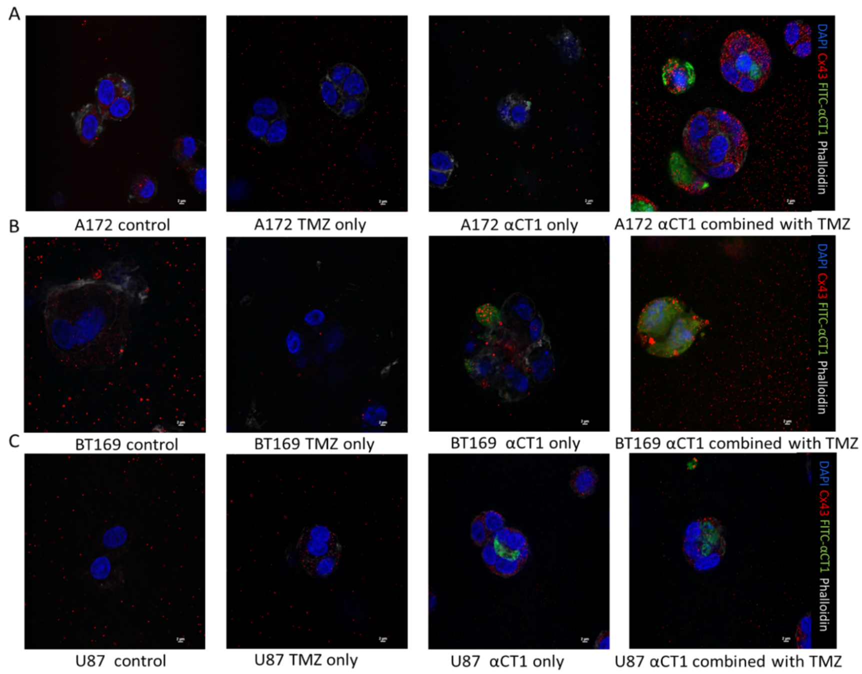

Figure 5. Immunofluorescence staining of GBM cells after treatment. A , A172 cells after treatment in four conditions: control (no drug or peptide), TMZ (100 µM), FITC-αCT1 (100 µM), and combination of 100 µM TMZ and 100 µM FITC-αCT1. **B** , BT169 cells after treatment in four conditions. **C** , U87 cells after treatment in four conditions. Blue, DAPI; Green, FITC- αCT1; Red, N-terminal Cx43; Gray, Phalloidin.

3.5. ἄλιδατιον οφ α῞Τ1-τεμοζολομιδε τρεατμεντ ιν πατιεντ-δεριεδ γλιοβλαστομα οργανοιδς

It has been established that studies using cell lines are limited (Fusenig et al., 2017). Cell lines often consist of a homogeneous population of cells that only represents a subset of the cells found in the heterogenous tumor in the patient. It has also been confirmed that some cell lines, namely the U87 cell line, are genetically and phenotypically different from the original cells obtained from patients many years ago (Allen et al., 2016). To partially address this issue, we used the BT169 cell line which is not immortalized and is cultured in conditions that enhance the formation of a heterogeneous population. Even so, we sought to validate that the combinatorial treatment of αCT1 and TMZ is effective in a patient derived GBM cell population.

The highest concentration of TMZ (1000 µM) killed most of the cells in our patient-derived cell population even without αCT1 (**Figure 6**). However, TMZ only was ineffective at lower concentrations (10 µM and 100 µM). Combinatorial treatment with αCT1 and TMZ resulted in significant decreases in cell viability in the TMZ 100 µM group. Interestingly, there was also a significant decrease of viability in the αCT1=100

μM, TMZ=0 condition, again indicating that αCT1 also induces other cellular changes in some subsets of GBM cells.

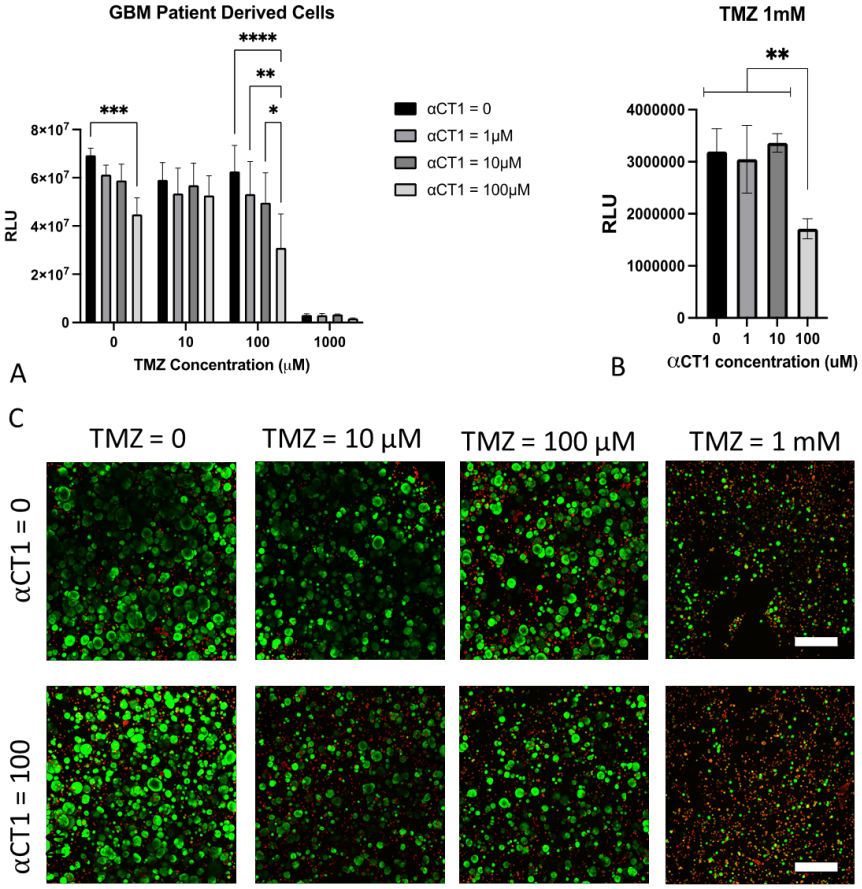

Figure 6. ATP assay data and LIVE/DEAD images of patient derived GBM cells. A, patient derived GBM cell viability after treatment with TMZ at 0, 10, 100, or 1000 μM alone or in combination with αCT1 at concentrations of 0, 1, 10, 100 μM. **B** , patient derived GBM cell ATP data responding to TMZ at 1000 μM alone or in combination with αCT1 at concentrations of 0, 1, 10, 100 μM. **C** , LIVE/DEAD images of patient derived cells after the treatment. Green – Calcein AM-stained viable cells; Red – Ethidium homodimer-1-stained dead cell nuclei. Treatment with lower concentrations of αCT1 (1 and 10 μM) can be found in Supplemental Figure 7. Scale bar – 250 μm.

4. Discussion

Connexin 43 (Cx43) is a member of transmembrane proteins that are responsible in part for intercellular communication via gap junctions. Recent studies have indicated that Cx43 controls the response of GBM cells to TMZ through various mechanisms, such as modulating mitochondrial apoptosis, and activating P13K signaling (Gielen et al., 2013; Munoz et al., 2014; Pridham et al., 2022). Pridham *et al.*have also shown that expression of Cx43 protein in high-grade glioma is higher than other connexins (Pridham et al., 2022). They also show that high levels of Cx43 mRNA were associated with poor prognosis of GBM patients (Pridham et al., 2022). αCT1 is a mimetic peptide of the Cx43 C-terminal and can inhibit Cx43 hemichannel functions (Montgomery et al., 2021). Therefore, we hypothesized that combinatorial treatment that consists of αCT1 peptide, which inhibits Cx43 hemichannel function, and TMZ could be used to sensitize GBM to TMZ.

To test this hypothesis, we chose to use a 3-dimensional *in vitro*culture system to model the GBM microenvironment. Traditional 2D cell culture is commonly used in research; however, it has limitations due to inaccurately representing tissue cells in vitro (Costa et al., 2016). The brain's extracellular matrix (ECM) is a macromolecular network of proteins and polysaccharides that acts as "scaffolding" in which neurons, glia, and other cells of the brain reside. ECM provides cells structural support and has crucial biomechanical and biochemical functions that regulate cell behaviors. The composition of the ECM is specific for each tissue type (Frantz et al., 2010). The brain's ECM is primarily composed of glycosaminoglycans (e.g., hyaluronan), proteoglycans, and glycoproteins, and contains low levels of fibrous proteins (e.g., collagen, fibronectin, and vitronectin) (Simsa et al., 2021). Hydrogels can be used to mimic the mechanical and biochemical properties of tumor ECM and could serve as a better model than conventional 2D tumor models (Hoarau-Véchot et al., 2018). Thus, in this study, to investigate how GBM responds to the drug candidate treatment, a 3D organoid model was used to mimic brain ECM. Our lab uses a UV-crosslinked hydrogel composed of hyaluronic acid and gelatin to mimic the high HA content in brain ECM and simulate mechanical properties of the native brain tissue. We have previously shown that this hydrogel supports the growth of GBM cells (Maloney et al., 2020; Sivakumar et al., 2017).

Initial experiments conducted in this study were done using several GBM cell lines. While cell lines are not always the best models of native tumors, the cell lines chosen represent distinct GBM tumor populations and allowed us to easily test this novel treatment methodology before working with valuable patient tumor samples. We chose to use 3 cell lines (A172, U87 MG, and BT169) because they represent slightly different populations of GBM tumor cells. The U87 MG cell line was isolated from malignant gliomas from human brain tissue (ATCC HTB-14). U87 MG cells have an epithelial-like morphology. The A172 cell line was isolated from glioblastoma from human brain tissue (ATCC(r) CRL-1620$^{\mathrm{TM}}$). While not perfect representations of previously defined clinical GBM subtypes, we have used U87 MG and A172 cell lines previously to represent different populations of GBM cells based on their different genetic profiles (Sivakumar et al., 2020). GSCs have the capacity to self-renew and differentiate into heterogeneous cell populations. This has been indicated as a possible driver of tumor recurrence and chemo-resistance. The BT169 cell line was used to represent a GSC GBM subpopulation. The cells form neutrosphere structures in tissue culture, which is an experimentally defined property of GSC (Ahmed et al., 2013). Thus, therapeutic methods that effectively target this GSC-like population are of utmost interest in our peptide-TMZ study. BT169 is MGMT promoter methylated, EGFR wild-type, PTEN heterozygous mutant, TP53 wild-type, IDH wild-type (ATCC$^{(\mathrm{r})}$ CRL-3413). Previous studies have shown that MGMT is associated with GBM resistance to alkylating agents such as TMZ, and methylation of the MGMT promotor is suggested to sensitize GBM to TMZ (Binabaj et al., 2018; Donson et al., 2007). Cristofano et al., demonstrated that PTEN heterozygous mice display hyperplastic features as well as high tumor incidence, which indicates that PTEN mutation may promote tumor progression (Di Cristofano et al., 1999). Nevertheless, Shen et al., demonstrated that wild-type IDH promotes primary GBM progression. Based on these indicators, we would predict a mixed response to TMZ (Shen et al., 2020).

Structural studies have shown that αCT1 directly interacts with a short α-helical sequence along the Cx43 C-terminal called H2 domain of Cx43 (Jiang et al., 2019). αCT11 is a 9-mer peptide variant of αCT1. Because αCT11 lacks the same cell penetration sequence as αCT1, it's likely that αCT11 isn't taken up by cells (Jiang et al., 2019). We have shown that the 3 GBM cell lines tested do not respond to treatment with αCT11 and TMZ (**Figure 2**). However, some cell lines, A172 and BT169, do respond to combination treatment with αCT11 and TMZ at certain concentrations (**Figure 3 and 4**). Our patient derived cells show decreased viability in αCT1+TMZ combination treatments (**Figure 6**). These results indicate that the combination treatment is effective on certain populations of cells. It is hypothesized that the GSC population present in the BT169 cells and patient derived cell population are sensitive to the combination. Specific population response will be investigated in future studies.

We used high resolution confocal imaging to begin investigating the possible mechanism of action of αCT1 and TMZ in combination. It was observed that in A172 and BT169s that αCT1 without TMZ induced significant changes in cell viability so we were interested to see if any changes would also be observed in

this condition. Immunofluorescent imaging shows that the Cx43 aggregates increased in A172 and BT169 cell lines significantly only after the combinatorial treatment, whereas the Cx43 aggregates number in the U87 cell line only increased slightly (**Figure 5**), which could explain why the combinatorial treatment in A172 and BT169 cell lines works better. These imaging studies will serve as a springboard for future super resolution studies to further evaluate the mechanism of action in order to design an effective treatment regimen.

Much of this study utilized tumor cell lines, and these cell lines do not accurately mimic the cellular heterogeneity of GBM. However, they serve as useful tools with which to begin exploring the utility of Cx43 inhibition in GBM. Importantly, we did also include experiments utilized a patient-derived tumor population, that does retain the heterogeneity of GBM, including preservation of glioma stem cell populations, which often contribute to the cell populations that are resistant to TMZ. In future work, we wish to expand our drug studies to patient-derived tumor organoids derived from multiple GBM patients. This will provide us with a better sense of the clinical utility of this treatment approach. In addition, we plan to embed GBM organoids within an *in vitro*microfluidic blood-brain barrier model, testing systemic versus local delivery of both TMZ and αCT1. This system will provide a more complex, and physiologically accurate model system of GBM, while retaining the use of human cells.

In conclusion, the studies presented here demonstrate potential to treat GBM using a combinatorial treatment with Cx43 mimetic peptide αCT1 and TMZ. Studies were conducted using 3D tumor organoids which accurately mimic the *in vivo* tumor microenvironment. The platform allows for high throughput screening of various treatment concentrations and high-resolution imaging to study mechanisms of action. Further studies are under way to optimize the treatment and design effective delivery vehicles.

Acknowledgements:

A.S acknowledges funding from NIH grants R21CA229027 and R21CA263137, the Pelotonia Foundation, and the Ohio State University Comprehensive Cancer Center. TJD and MMT acknowledge support from the Pelotonia Graduate Fellowship Program. JC acknowledges support from the OSU College of Engineering Undergraduate Research Distinction Program. MV acknowledges funding from a Research Scholar Grant RSG-18-066-01-TBG from the American Cancer Society, NIH grant R21CA250118, and funds from The Ohio State University Comprehensive Cancer Center/Department of Radiation Oncology The authors thank Dr. Jeremy Rich (University of Pittsburgh) for the kind gift of the GBM 3691.

Conflicts of Interest:

The authors have no conflicts of interest to disclose.

References:

Ahmed, A. U., Auffinger, B., & Lesniak, M. S. (2013). Understanding glioma stem cells: rationale, clinical relevance and therapeutic strategies. *Expert Review of Neurotherapeutics* , *13* (5), 545-555. https://doi.org/10.1586/ern.13.42

Allen, M., Bjerke, M., Edlund, H., Nelander, S., & Westermark, B. (2016). Origin of the U87MG glioma cell line: Good news and bad news.*Science Translational Medicine* , *8* (354), 354re353-354re353. https://doi.org/10.1126/scitranslmed.aaf6853

Auffinger, B., Spencer, D., Pytel, P., Ahmed, A. U., & Lesniak, M. S. (2015). The role of glioma stem cells in chemotherapy resistance and glioblastoma multiforme recurrence. *Expert Rev Neurother* ,*15* (7), 741-752. https://doi.org/10.1586/14737175.2015.1051968

Binabaj, M. M., Bahrami, A., ShahidSales, S., Joodi, M., Joudi Mashhad, M., Hassanian, S. M., Anvari, K., & Avan, A. (2018). The prognostic value of MGMT promoter methylation in glioblastoma: A meta-analysis of clinical trials. *J Cell Physiol* , *233* (1), 378-386. https://doi.org/10.1002/jcp.25896

Costa, E. C., Moreira, A. F., de Melo-Diogo, D., Gaspar, V. M., Carvalho, M. P., & Correia, I. J. (2016).

3D tumor spheroids: an overview on the tools and techniques used for their analysis.*Biotechnol Adv* , *34* (8), 1427-1441. https://doi.org/10.1016/j.biotechadv.2016.11.002

Devarasetty, M., Dominijanni, A., Herberg, S., Shelkey, E., Skardal, A., & Soker, S. (2020). Simulating the human colorectal cancer microenvironment in 3D tumor-stroma co-cultures in vitro and in vivo.*Sci Rep* , *10* (1), 9832. https://doi.org/10.1038/s41598-020-66785-1

Di Cristofano, A., Kotsi, P., Peng, Y. F., Cordon-Cardo, C., Elkon, K. B., & Pandolfi, P. P. (1999). Impaired Fas response and autoimmunity in Pten+/- mice. *Science* , *285* (5436), 2122-2125. https://doi.org/10.1126/science.285.5436.2122

Dominijanni, A. J., Devarasetty, M., Forsythe, S. D., Votanopoulos, K. I., & Soker, S. (2021). Cell Viability Assays in Three-Dimensional Hydrogels: A Comparative Study of Accuracy. *Tissue Engineering Part C: Methods* , *27* (7), 401-410. https://doi.org/10.1089/ten.tec.2021.0060

Donson, A. M., Addo-Yobo, S. O., Handler, M. H., Gore, L., & Foreman, N. K. (2007). MGMT promoter methylation correlates with survival benefit and sensitivity to temozolomide in pediatric glioblastoma. *Pediatr Blood Cancer* , *48* (4), 403-407. https://doi.org/10.1002/pbc.20803

Fedele, M., Cerchia, L., Pegoraro, S., Sgarra, R., & Manfioletti, G. (2019). Proneural-Mesenchymal Transition: Phenotypic Plasticity to Acquire Multitherapy Resistance in Glioblastoma. *Int J Mol Sci* ,*20* (11). https://doi.org/10.3390/ijms20112746

Forsythe, S., Mehta, N., Devarasetty, M., Sivakumar, H., Gmeiner, W., Soker, S., Votanopoulos, K., & Skardal, A. (2019). Development of a Colorectal Cancer 3D Micro-tumor Construct Platform From Cell Lines and Patient Tumor Biospecimens for Standard-of-Care and Experimental Drug Screening. *Ann Biomed Eng* . https://doi.org/10.1007/s10439-019-02269-2

Frantz, C., Stewart, K. M., & Weaver, V. M. (2010). The extracellular matrix at a glance. *Journal of Cell Science* , *123* (24), 4195-4200. https://doi.org/10.1242/jcs.023820

Fusenig, N. E., Capes-Davis, A., Bianchini, F., Sundell, S., & Lichter, P. (2017). The need for a worldwide consensus for cell line authentication: Experience implementing a mandatory requirement at the International Journal of Cancer. *PLOS Biology* , *15* (4), e2001438. https://doi.org/10.1371/journal.pbio.2001438

Gielen, P. R., Aftab, Q., Ma, N., Chen, V. C., Hong, X., Lozinsky, S., Naus, C. C., & Sin, W. C. (2013). Connexin43 confers Temozolomide resistance in human glioma cells by modulating the mitochondrial apoptosis pathway. *Neuropharmacology* , *75* , 539-548. https://doi.org/10.1016/j.neuropharm.2013.05.002

Grek, C. L., Sheng, Z., Naus, C. C., Sin, W. C., Gourdie, R. G., & Ghatnekar, G. G. (2018). Novel approach to temozolomide resistance in malignant glioma: connexin43-directed therapeutics. *Curr Opin Pharmacol* , *41* , 79-88. https://doi.org/10.1016/j.coph.2018.05.002

Heimberger, A. B., Crotty, L. E., Archer, G. E., Hess, K. R., Wikstrand, C. J., Friedman, A. H., Friedman, H. S., Bigner, D. D., & Sampson, J. H. (2003). Epidermal growth factor receptor VIII peptide vaccination is efficacious against established intracerebral tumors. *Clin Cancer Res* , *9* (11), 4247-4254. https://www.ncbi.nlm.nih.gov/pubmed/14519652

Hoarau-Véchot, J., Rafii, A., Touboul, C., & Pasquier, J. (2018). Halfway between 2D and Animal Models: Are 3D Cultures the Ideal Tool to Study Cancer-Microenvironment Interactions? *Int J Mol Sci* ,*19* (1). https://doi.org/10.3390/ijms19010181

Jiang, J., Hoagland, D., Palatinus, J. A., He, H., Iyyathurai, J., Jourdan, L. J., Bultynck, G., Wang, Z., Zhang, Z., Schey, K., Poelzing, S., McGowan, F. X., & Gourdie, R. G. (2019). Interaction of α Carboxyl Terminus 1 Peptide With the Connexin 43 Carboxyl Terminus Preserves Left Ventricular Function After Ischemia-Reperfusion Injury. *Journal of the American Heart Association* , *8* (16), e012385. https://doi.org/10.1161/JAHA.119.012385

Lee, S. Y. (2016). Temozolomide resistance in glioblastoma multiforme. *Genes Dis* , *3* (3), 198-210. https://doi.org/10.1016/j.gendis.2016.04.007

Malkki, H. (2016). Trial Watch: Glioblastoma vaccine therapy disappointment in Phase III trial. *Nat Rev Neurol* , *12* (4), 190. https://doi.org/10.1038/nrneurol.2016.38

Maloney, E., Clark, C., Sivakumar, H., Yoo, K., Aleman, J., Rajan, S. A. P., Forsythe, S., Mazzocchi, A., Laxton, A. W., Tatter, S. B., Strowd, R. E., Votanopoulos, K. I., & Skardal, A. (2020). Immersion Bioprinting of Tumor Organoids in Multi-Well Plates for Increasing Chemotherapy Screening Throughput. *Micromachines (Basel)* , *11* (2). https://doi.org/10.3390/mi11020208

Mazzocchi, A., Devarasetty, M., Herberg, S., Petty, W. J., Marini, F., Miller, L., Kucera, G., Dukes, D. K., Ruiz, J., Skardal, A., & Soker, S. (2019). Pleural Effusion Aspirate for use in 3D Lung Cancer Modeling and Chemotherapy Screening. *ACS Biomater Sci Eng* , *5* (4), 1937-1943. https://doi.org/10.1021/acsbiomaterials.8b01356

Mazzocchi, A. R., Rajan, S. A. P., Votanopoulos, K. I., Hall, A. R., & Skardal, A. (2018). In vitro patient-derived 3D mesothelioma tumor organoids facilitate patient-centric therapeutic screening. *Sci Rep* , *8* (1), 2886. https://doi.org/10.1038/s41598-018-21200-8

Montgomery, J., Richardson, W. J., Marsh, S., Rhett, J. M., Bustos, F., Degen, K., Ghatnekar, G. S., Grek, C. L., Jourdan, L. J., Holmes, J. W., & Gourdie, R. G. (2021). The connexin 43 carboxyl terminal mimetic peptide αCT1 prompts differentiation of a collagen scar matrix in humans resembling unwounded skin. *Faseb j* , *35* (8), e21762. https://doi.org/10.1096/fj.202001881R

Munoz, J. L., Rodriguez-Cruz, V., Greco, S. J., Ramkissoon, S. H., Ligon, K. L., & Rameshwar, P. (2014). Temozolomide resistance in glioblastoma cells occurs partly through epidermal growth factor receptor-mediated induction of connexin 43. *Cell Death & Disease* , *5* (3), e1145-e1145. https://doi.org/10.1038/cddis.2014.111

Murphy, S. F., Varghese, R. T., Lamouille, S., Guo, S., Pridham, K. J., Kanabur, P., Osimani, A. M., Sharma, S., Jourdan, J., Rodgers, C. M., Simonds, G. R., Gourdie, R. G., & Sheng, Z. (2016). Connexin 43 Inhibition Sensitizes Chemoresistant Glioblastoma Cells to Temozolomide. *Cancer Res* , *76* (1), 139-149. https://doi.org/10.1158/0008-5472.CAN-15-1286

Pridham, K. J., Shah, F., Hutchings, K. R., Sheng, K. L., Guo, S., Liu, M., Kanabur, P., Lamouille, S., Lewis, G., Morales, M., Jourdan, J., Grek, C. L., Ghatnekar, G. G., Varghese, R., Kelly, D. F., Gourdie, R. G., & Sheng, Z. (2022). Connexin 43 confers chemoresistance through activating PI3K. *Oncogenesis* , *11* (1), 2. https://doi.org/10.1038/s41389-022-00378-7

Roberts, R., Smyth, J. W., Will, J., Roberts, P., Grek, C. L., Ghatnekar, G. S., Sheng, Z., Gourdie, R. G., Lamouille, S., & Foster, E. J. (2020). Development of PLGA nanoparticles for sustained release of a connexin43 mimetic peptide to target glioblastoma cells. *Mater Sci Eng C Mater Biol Appl* , *108* , 110191. https://doi.org/10.1016/j.msec.2019.110191

Rubenstein, J. L., Li, J., Chen, L., Advani, R., Drappatz, J., Gerstner, E., Batchelor, T., Krouwer, H., Hwang, J., Auerback, G., Kadoch, C., Lowell, C., Munster, P., Cha, S., Shuman, M. A., & Damon, L. E. (2013). Multicenter phase 1 trial of intraventricular immunochemotherapy in recurrent CNS lymphoma. *Blood* , *121* (5), 745-751. https://doi.org/10.1182/blood-2012-07-440974

Rybinski, B., & Yun, K. (2016). Addressing intra-tumoral heterogeneity and therapy resistance. *Oncotarget* , *7* (44), 72322-72342. https://doi.org/10.18632/oncotarget.11875

Segerman, A., Niklasson, M., Haglund, C., Bergstrom, T., Jarvius, M., Xie, Y., Westermark, A., Sonmez, D., Hermansson, A., Kastemar, M., Naimaie-Ali, Z., Nyberg, F., Berglund, M., Sundstrom, M., Hesselager, G., Uhrbom, L., Gustafsson, M., Larsson, R., Fryknas, M., . . . Westermark, B. (2016). Clonal Variation in Drug

and Radiation Response among Glioma-Initiating Cells Is Linked to Proneural-Mesenchymal Transition. *Cell Rep* , *17* (11), 2994-3009. https://doi.org/10.1016/j.celrep.2016.11.056

Shen, X., Wu, S., Zhang, J., Li, M., Xu, F., Wang, A., Lei, Y., & Zhu, G. (2020). Wild-type IDH1 affects cell migration by modulating the PI3K/AKT/mTOR pathway in primary glioblastoma cells. *Mol Med Rep* ,*22* (3), 1949-1957. https://doi.org/10.3892/mmr.2020.11250

Simsa, R., Rothenbücher, T., Gürbüz, H., Ghosheh, N., Emneus, J., Jenndahl, L., Kaplan, D. L., Bergh, N., Serrano, A. M., & Fogelstrand, P. (2021). Brain organoid formation on decellularized porcine brain ECM hydrogels. *PLoS ONE* , *16* (1), e0245685. https://doi.org/10.1371/journal.pone.0245685

Sivakumar, H., Devarasetty, M., Kram, D. E., Strowd, R. E., & Skardal, A. (2020). Multi-Cell Type Glioblastoma Tumor Spheroids for Evaluating Sub-Population-Specific Drug Response. *Frontiers in bioengineering and biotechnology* , *8* , 538663-538663. https://doi.org/10.3389/fbioe.2020.538663

Sivakumar, H., Strowd, R., & Skardal, A. (2017). Exploration of Dynamic Elastic Modulus Changes on Glioblastoma Cell Populations with Aberrant EGFR Expression as a Potential Therapeutic Intervention Using a Tunable Hyaluronic Acid Hydrogel Platform. *Gels* , *3* (3). https://doi.org/10.3390/gels3030028

Sottoriva, A., Spiteri, I., Piccirillo, S. G., Touloumis, A., Collins, V. P., Marioni, J. C., Curtis, C., Watts, C., & Tavare, S. (2013). Intratumor heterogeneity in human glioblastoma reflects cancer evolutionary dynamics. *Proc Natl Acad Sci U S A* , *110* (10), 4009-4014. https://doi.org/10.1073/pnas.1219747110

Stupp, R., Mason, W. P., van den Bent, M. J., Weller, M., Fisher, B., Taphoorn, M. J., Belanger, K., Brandes, A. A., Marosi, C., Bogdahn, U., Curschmann, J., Janzer, R. C., Ludwin, S. K., Gorlia, T., Allgeier, A., Lacombe, D., Cairncross, J. G., Eisenhauer, E., Mirimanoff, R. O., . . . National Cancer Institute of Canada Clinical Trials, G. (2005). Radiotherapy plus concomitant and adjuvant temozolomide for glioblastoma. *N Engl J Med* , *352* (10), 987-996. https://doi.org/10.1056/NEJMoa043330

Swartz, A. M., Li, Q. J., & Sampson, J. H. (2014). Rindopepimut: a promising immunotherapeutic for the treatment of glioblastoma multiforme. *Immunotherapy* , *6* (6), 679-690. https://doi.org/10.2217/imt.14.21

Taal, W., Oosterkamp, H. M., Walenkamp, A. M., Dubbink, H. J., Beerepoot, L. V., Hanse, M. C., Buter, J., Honkoop, A. H., Boerman, D., de Vos, F. Y., Dinjens, W. N., Enting, R. H., Taphoorn, M. J., van den Berkmortel, F. W., Jansen, R. L., Brandsma, D., Bromberg, J. E., van Heuvel, I., Vernhout, R. M., . . . van den Bent, M. J. (2014). Single-agent bevacizumab or lomustine versus a combination of bevacizumab plus lomustine in patients with recurrent glioblastoma (BELOB trial): a randomised controlled phase 2 trial. *Lancet Oncol* , *15* (9), 943-953. https://doi.org/10.1016/S1470-2045(14)70314-6

Tang, C., Guo, J., Chen, H., Yao, C. J., Zhuang, D. X., Wang, Y., Tang, W. J., Ren, G., Yao, Y., Wu, J. S., Mao, Y., & Zhou, L. F. (2015). Gene mutation profiling of primary glioblastoma through multiple tumor biopsy guided by 1H-magnetic resonance spectroscopy. *Int J Clin Exp Pathol* , *8* (5), 5327-5335. https://www.ncbi.nlm.nih.gov/pubmed/26191234

Verhaak, R. G., Hoadley, K. A., Purdom, E., Wang, V., Qi, Y., Wilkerson, M. D., Miller, C. R., Ding, L., Golub, T., Mesirov, J. P., Alexe, G., Lawrence, M., O'Kelly, M., Tamayo, P., Weir, B. A., Gabriel, S., Winckler, W., Gupta, S., Jakkula, L., . . . Cancer Genome Atlas Research, N. (2010). Integrated genomic analysis identifies clinically relevant subtypes of glioblastoma characterized by abnormalities in PDGFRA, IDH1, EGFR, and NF1. *Cancer Cell* , *17* (1), 98-110. https://doi.org/10.1016/j.ccr.2009.12.020

Votanopoulos, K. I., Forsythe, S., Sivakumar, H., Mazzocchi, A., Aleman, J., Miller, L., Levine, E., Triozzi, P., & Skardal, A. (2019). Model of Patient-Specific Immune-Enhanced Organoids for Immunotherapy Screening: Feasibility Study. *Ann Surg Oncol* . https://doi.org/10.1245/s10434-019-08143-8

Votanopoulos, K. I., Mazzocchi, A., Sivakumar, H., Forsythe, S., Aleman, J., Levine, E. A., & Skardal, A. (2019). Appendiceal Cancer Patient-Specific Tumor Organoid Model for Predicting Chemotherapy Efficacy Prior to Initiation of Treatment: A Feasibility Study.*Ann Surg Oncol* , *26* (1), 139-147.

https://doi.org/10.1245/s10434-018-7008-2

Votanopoulos, K. I., & Skardal, A. (2020). ASO Author Reflections: Co-cultured Lymph Node and Tumor Organoids as a Platform for the Creation of Adaptive Immunity and Predict Response to Immunotherapy. *Ann Surg Oncol* . https://doi.org/10.1245/s10434-020-08351-7

Zhang, J., Stevens, M. F., & Bradshaw, T. D. (2012). Temozolomide: mechanisms of action, repair and resistance. *Curr Mol Pharmacol* ,*5* (1), 102-114. https://doi.org/10.2174/1874467211205010102